Title

Wnt signaling dynamics in head and neck squamous cell cancer tumor-stroma interactions

Journal

Molecular Carcinogenesis, 58(3)

ISSN

0899-1987

Authors

Le, Phuong N
Keysar, Stephen B
Miller, Bettina
et al.

Publication Date

2019-03-01

DOI

10.1002/mc.22937

Peer reviewed

HHS Public Access

Author manuscript

Mol Carcinog. Author manuscript; available in PMC 2020 March 01.

Published in final edited form as:

Mol Carcinog. 2019 March ; 58(3): 398–410. doi:10.1002/mc.22937.

Wnt signaling dynamics in head and neck squamous cell cancer tumor-stroma interactions

Phuong N. Le[1], **Stephen B. Keysar**[1], **Bettina Miller**[1], **Justin R. Eagles**[1], **Tugs-Saikhan Chimed**[1], **Julie Reisinger**[1], **Karina E. Gomez**[1], **Cera Nieto**[1], **Brian C. Jackson**[1], **Hilary L. Somerset**[2], **J. Jason Morton**[1], **Xiao-Jing Wang**[2,3], and **Antonio Jimeno**[1,3]

[1]Division of Medical Oncology, Department of Medicine, University of Colorado Denver School of Medicine (UCDSOM), CO, 80045.

[2]Department of Pathology, UCDSOM, CO, 80045.

[3]Gates Center for Regenerative Medicine, UCDSOM, CO, 80045.

Abstract

Wnt pathway activation maintains the cancer stem cell (CSC) phenotype and promotes tumor progression, making it an attractive target for anti-cancer therapy. Wnt signaling at the tumor and tumor microenvironment (TME) front have not been investigated in depth in head and neck squamous cell carcinoma (HNSCC). In a cohort of 48 HNSCCs, increased Wnt signaling, including Wnt genes (*AXIN2*, *LGR6*, *WISP1*) and stem cell factors (*RET*, *SOX5*, *KIT*), were associated with a more advanced clinical stage. Key Wnt pathway proteins were most abundant at the cancer epithelial-stromal boundary. To investigate these observations, we generated three pairs of cancer-cancer associated fibroblast (CAF) cell lines derived from the same HNSCC patients. 3D co-culture of cancer spheres and CAFs mimicked these *in vivo* interactions, and using these we observed increased expression of Wnt genes (e.g. *WNT3A*, *WNT7A*, *WNT16*) in both compartments. Of these Wnt ligands, we found Wnt3a, and less consistently Wnt16, activated Wnt signaling in both cancer cells and CAFs. Wnt activation increased CSC characteristics like sphere formation and invasiveness, which was further regulated by the presence of CAFs. Time lapse microscopy also revealed preferential Wnt activation of cancer cells. Wnt inhibitors, OMP-18R5 and OMP-54F28, significantly reduced growth of HNSCC patient-derived xenografts and suppressed Wnt activation at the tumor epithelial-stromal boundary. Taken together, our findings suggest that Wnt signaling is initiated in cancer cells which then activate CAFs, and in turn perpetuate a paracrine signaling loop. This suggests that targeting Wnt signaling in the TME is essential.

Corresponding Author Antonio Jimeno M.D., Ph.D., Professor of Medicine/Oncology, and Otolaryngology, University of Colorado Denver School of Medicine, 12801 East 17th Avenue, Room L18-8111, Aurora, CO 80045, USA, Antonio.Jimeno@ucdenver.edu.

Disclosures

The authors declare no conflict of interest and have no relevant disclosures.

Data and materials availability

Materials will be shared per the University of Colorado's Office for Technology Transfer policies and Institutional Review Board.

Keywords

Head and neck squamous cell cancer; Wnt signaling; Wnt3a; cancer stem cells; Sox2

1. INTRODUCTION

Over 63,000 people are diagnosed with head and neck squamous cell carcinoma (HNSCC) in the US each year [1], which is increasing due to a rise in human papillomavirus (HPV)-related cases [2]. Wnt signaling is vital in embryonic development [3] and consists of a canonical (β-catenin dependent) and two non-canonical pathways (Wnt/PCP, Wnt/calcium), which are inherently linked [4]. Wnt activation in cancer cells induces proliferative, invasive and stem cell-like phenotypes [5–8]. Briefly, when canonical Wnt is off, β-catenin is recruited to the destruction complex and phosphorylated [9], targeting it for ubiquitination and degradation [10]. However, when Wnt ligand binds the Frizzled (Fzd) receptor and LRP5/6 co-receptor [11,12], the destruction complex is inactivated through Axin degradation [13,14]. Lack of negative regulation allows unphosphorylated β-catenin to accumulate in the cytoplasm and translocate into the nucleus, where it interacts with TCF-LEF to activate target gene expression [15]. These multi-faceted roles make Wnt an efficient tumorigenic pathway, and it is commonly activated in HNSCC, breast, prostate and colorectal cancers [6,7,16,17]. However, the role of Wnt signaling in HNSCC is less well defined than in other cancers.

Similar to its crucial roles in development, Wnt signaling maintains key cancer stem cell (CSC) properties across multiple cancers [18–20], including HNSCC [7,8,20]. β-catenin expression correlates with poor prognosis in HNSCC patients, and its inhibition blocks tumor proliferation *in vivo* [7]. HNSCC CSC properties decrease following Wnt inhibition [21,22], and tumorigenic side population cells exhibit aberrant Wnt activation and generate larger and more invasive tumors [8,23]. Recently we demonstrated enrichment of Wnt signaling in highly tumorigenic HNSCC CSCs and that Sox2 increased expression of Wnt genes (e.g. *AXIN1, AXIN2*) [24], suggesting that Wnt and Sox2 are linked in their contribution to CSC maintenance.

TME compartments promote tumor growth, invasiveness, and resistance across tumor types [18,25,26], and preclinical studies targeting Wnt in the TME inhibited tumor growth [27]. Although the contribution of the TME to cancer has been brought to the forefront of tumor biology, how cancer cells use Wnt signaling to harness the tumor microenvironment (TME) and enable HNSCC growth, invasion and CSC maintenance has not been fully studied. Here we found Wnt expression correlated with HNSCC aggressiveness.

To elucidate Wnt signaling during the cancer epithelia-CAF interaction *in vitro*, we isolated paired cancer cells and cancer associated fibroblasts (CAFs), known to be a critical player in the TME [28], from the same patient to model an *in vivo* setting. We found that Wnt3a, known to be an “activating ligand” [29], and less frequently Wnt16, activated Wnt signaling in both cancer cells and CAFs. Activation increased the CSC phenotype and “primed” cancer cells’ invasive potential through transient upregulation of Twist1. Using time-lapse microscopy, we found that cancer cells are preferentially activated, and co-culture

experiments showed that cancer cells could initiate paracrine Wnt signaling with neighboring CAFs, suggesting a Wnt signaling loop and highlighting the need to target both compartments during therapy. Lastly, Wnt inhibitors suppressed proliferation of patient-derived xenografts (PDXs) by suppressing Wnt signaling at the cancer-TME interface. We also found targeting Wnt signaling specifically in the stroma was effective at inhibiting tumor initiation. Together, these findings indicate that Wnt increases CSC properties like invasiveness, sphere formation, and *in vivo* growth in HNSCC, and these tumor-promoting effects are enabled by the dynamics of the cancer-TME interaction.

2. METHODS

2.1. PDX generation and *in vivo* studies

Studies involving human subjects were approved by the Colorado Multiple Institutional Review Board (COMIRB #08–0552). The University of Colorado Institutional Animal Care and Use Committee (IACUC) approved all experiments involving mice. PDX generation and characterization was previously reported [30].

OMP-18R5 and OMP-54F28 (OncoMed) were provided under a Material Transfer Agreement. Therapy was delivered by intraperitoneal injection, biweekly at 20mg/kg, and tumors were measured twice weekly. Each treatment arm (vehicle, OMP-18R5, OMP-54F28) began treatment with a minimum of 10 tumors.

2.2. Cell lines

013C, 036C and 067C cells were derived from tumor tissue using RMK media (DMEM:F12 [3:1] with 10% FBS, Insulin [5μg/ml], EGF [10ng/ml], hydrocortisone [0.4μg/ml], transferrin [5μg/ml], penicillin [200units/mL], and streptomycin [200ug/mL]). 013CAF, 036CAF, and 067CAF were derived from tumor tissue in DMEM+10% FBS, penicillin (200units/mL), streptomycin (200ug/mL) and immortalized using SV40 LgT and hTERT expression.

2.3. RNA-seq analysis

RNA-seq processing and analysis were conducted as reported [24].

2.4. Fluorescence activated cell sorting (FACS) and flow cytometry

Analyses were conducted as reported [24].

2.5. CSC implantation *in vivo*

CSCs were sorted (FACS) into PBS+2% FBS, suspended in 1:1, DMEM+10% FBS:Matrigel (Corning) and injected into the flanks of nude mice. Tumor growth was monitored for up to 12 months.

2.6. Tumor sphere assay

Cell lines were plated in ultra-low attachment plates at a concentration of 1×10^5 (6-well plate) or 2.5×10^4 (24-well plate) per well. Media was supplemented 4- and 7-days following

cell seeding. Spheres were imaged (day 10 unless otherwise noted), counted and measured using a Zeiss Axio Observer Z1 inverted microscope (Zeiss software Rel. 4.8).

2.7. Matrigel coated invasion assay

Matrigel-coated 8μm pore 6-well inserts were purchased from Corning, and experiments were done according to manufacturer's instructions with few modifications. In TME invasion experiments, CAFs were added to the bottom well in DMEM+10% FBS. Invasion was quantified as cells/view at 5X magnification for 6 fields/insert. Experimental conditions were run in triplicate and experiments were repeated three times.

2.8. RNA isolation and gene expression

Gene expression analysis was previously described [24]. Briefly, PCR amplification and probe (Applied Biosystems) detection were accomplished using the StepOnePlus Real-Time PCR System (Applied Biosystems). All data are representative of experiments performed at least three times in triplicate.

2.9. Protein isolation and western blotting

Western blot analysis was conducted as described [24]. Antibodies and dilutions are listed in the Supplementary Materials.

2.10. Immunohistochemistry (IHC)

IHC analyses were performed as previously described [30]. Primary antibodies and dilutions are listed in the Supplementary Materials.

2.11. TOP-Flash, TOP-GFP and time lapse microscopy

For TOP-Flash, cells were seeded (7,500–10,000/well) in triplicate in 96-well plates and transfected with TOP-Flash, Fop-Flash or control luciferase plasmids. LiCl (20mM-40mM), rWnts and Wnt inhibitors (10mg/ml) are added on day 3. Luciferase activity was quantified on day 4 using Promega substrate according to manufacturer's instructions. TOP-GFP and FOP-GFP expressing cells were seeded at 15,000 total cells/well in 24-well plates and imaged on day 4 (6 images/treatment, quantified as GFP+ cells/view). For time lapse microscopy, images were taken every 15–20min on a Zeiss Axio Observer Z1 inverted microscope, equipped with an incubation chamber with regulated temperature, humidity and CO_2. Time of TOP-GFP activation was analyzed without threshold modification for rWnt3a experiments and with automatic software thresholding in media transfer experiments.

2.12. Statistics

In vitro and *in vivo* (using ≥5 mice/group) experiments were compared with a two-group t-test. Fisher exact tests were used to compare CSC implantation data. Calculations were done using GraphPad Prism version 7.0. Data are represented graphically as mean±SEM.

3. RESULTS

3.1. Wnt expression correlates with advanced tumor stage in HNSCC

To explore the relationship between Wnt activation and HNSCC progression we first compared the transcriptomes between early and advanced stage HNSCC tumors in our PDX bank [30]. Gene set enrichment analysis (GSEA) comparing 1) 25 relapsed vs. 18 primary tumors and 2) 25 cases with advanced nodal stage or metastases (≥N2 and/or M1) vs. 23 early stage tumors showed that relapsed and advanced tumors both had enrichment of Hallmark "Wnt/β-catenin signaling" (P=0.041), as well as enrichment of "E2F targets" (P<0.001) in relapsed cases (Supplementary Fig. S1A). Genes significantly (>2-fold change, P<0.05) upregulated in relapsed and advanced cases included the Wnt-related *LGR6*, *WISP1*, and *AXIN2*, which is a marker of canonical Wnt activation. We also observed enrichment of genes related to therapeutic resistance (*ADAMTS13*) and CSC signaling (*KIT, RET, SOX5*) (Supplementary Fig. S1A).

Having confirmed Wnt activation in HNSCC progression, we assessed key Wnt proteins and markers of Wnt activation by IHC in patient tumor tissue. While advanced stage tumors had 8 of the 10 highest staining values of Axin2, this enrichment was not statistically significant (P=.117) (Fig. 1A). However, Wnt3a and Axin2 expression were closely associated with β-catenin staining, which was predominantly located in the tumor epithelial cells adjacent to unstained stroma (Fig. 1A).

3.2. Establishing patient-matched cancer-CAF cell line pairs to investigate Wnt signaling in HNSCC

We have previously reported the loss of human stroma in our established PDX model [30]. Therefore, in order to study Wnt in HNSCC promotion, as well as characterizing its activity in CAFs, we isolated three "pairs" (013, 036, 067) of cancer cell lines (C) and cancer associated fibroblasts (CAFs) from the same patient tumors (Supplementary Table S1). CAFs were immortalized by expression of hTERT and SV40 Large T antigen [31] (Supplementary Fig. S1B–S1C). Tissue of origin was confirmed by short tandem repeat (STR) analysis and cancer cells implanted into mice formed tumors similar in morphology to the originating patient tumor and PDX model (Supplementary Fig. S1D).

First, we compared baseline expression of Wnt-related genes across our cancer and CAF cell lines. *WNT2* mRNA was not detectable in cancer cells, but *WNT2* was expressed in 013CAFs and 067CAFs. Expression of *WNT3A*, *WNT7A* and *WNT16* was highest in 067C, but expression of downstream Wnt targets (*AXIN2*, *NFAT1/NFAT2C*) was low in 067C (Supplementary Fig. S2A). We also analyzed protein levels of key Wnt components, EMT factors and CSC-related genes, finding that Wnt3a was highly expressed in 013C and 067C, while Wnt16 was highest in CAFs (Supplementary Fig. S2B). We next modeled Wnt signaling during cancer-CAF interactions *in vitro* by growing these "pairs" together in 3D co-culture and making comparisons to cancer cells and CAFs seeded alone (control). Following co-culture, Wnt ligand expression increased, which occurred more consistently in CAFs. Co-culture also increased *AXIN2* and *NFAT1/NFAT2C* expression in 067C but not

013C and 036C, and *NFAT1/NFAT2C* was upregulated in all three CAF lines (Supplementary Fig. S2C).

3.3. Exogenous Wnt3a activates Wnt signaling in cancer and CAF lines

Several studies have shown that tumor maintenance is dependent on continuous Wnt signaling [32,33]. Therefore, we aimed to model Wnt activation observed in tumor samples through exogenous expression (Fig. 1B, Supplementary Fig. S3) or addition of recombinant Wnt ligands in both cancer and CAF cultures. We screened candidate ligands identified in subsection 3.2 for canonical Wnt/β-catenin activation using the TOP-Flash reporter assay, which contains seven copies of TCF/LEF binding sites that control expression of luciferase. Here, we use this as an on/off reporter and we observed high variation in activation (fold change) among the recombinant ligands tested (rWnt3a, rWnt2, rWnt7a, rWnt16). However, we found that rWnt3a, as well as exogenous Wnt3a expression, activated the TOP-Flash reporter in 013C. We observed moderate activation in 036C and very limited activation in 067C at high doses of rWnt3a (500ng/mL), and luciferase was undetectable in both cell lines when overexpressing Wnt3a (Fig. 1C, Supplementary Fig. S4A–S4B). Activation of TOP-Flash by Wnt3a (recombinant ligand or forced expression) in 013C cells was blocked by Wnt inhibitors, OMP-18R5 and OMP-54F28 (Fig. 1C, Supplementary Fig. S4C). OMP-54F28 is an immunoglobulin G1 (IgG1) region fused with a Fzd receptor that binds and sequesters Wnt ligands [34,35], while OMP-18R5 is a monoclonal antibody that binds to multiple Fzds, including Fzd1, Fzd2, Fzd5 and Fzd8, thus blocking ligand binding [29].

Addition of rWnt3a increased Axin2 or Nfat1 protein levels in 013C and 036C, as well as 13CAF, consistent with TOP-Flash activity (Supplementary Fig. S4D). We observed a consistent increase in *AXIN2*/Axin2 in $013C^{Wnt3a}$ and $036C^{Wnt3a}$ (Supplementary Fig. S5A–S5D), confirming downstream Wnt activation. In $013C^{Wnt3a}$ we also observed significant increases in *TWIST1*, *ZEB1*, and *CCND1,* genes involved in EMT (TWIST1 and ZEB1) and proliferation (CCND1), as well as *NFAT1/NFAT2C*, a known target of non-canonical Wnt (Supplementary Fig. S5A). Increased protein expression of Axin2, Nfat1 and Cyclin D1 were confirmed (Supplementary Fig. S5B). We did not detect luciferase activity using TOP-Flash in 036C and 067C cells overexpressing Wnt3a, and we therefore replaced the high-throughput luciferase readout with TOP-GFP, allowing for the detection of single GFP-positive cells. We confirmed Wnt activation in cancer cells containing the TOP-GFP reporter by adjacent cancer cells (co-cultured) exogenously expressing Wnt3a. Wnt activation (TOP-GFP), assessed as on/off by the presence of GFP-positive cells, was observed in $013C^{Wnt3a}$ and $036C^{Wnt3a}$, but not in $067C^{Wnt3a}$, regardless of cell ratio (1:1, 1:4 and 1:10 TOP-GFP cells: overexpressing cells) or incubation time (Fig. 1D, Supplementary Fig. S6A). Interestingly, in $067C^{Wnt3a}$, where activation was not detected by TOP-Flash/GFP, we observed a trend towards decreased *AXIN2* and significant decreases in *ZEB1* and *NFAT1/NFAT2C* (Supplementary Fig. S5A).

3.4. Wnt3a in CAFs activates signaling in adjacent cancer cells

Wnt activation occurs both via autocrine and/or paracrine signaling [4,34,36]. In subsection 3.3 we demonstrated paracrine signaling wherein cancer cells expressing Wnt3a activate Wnt in neighboring cells containing TOP-GFP. We next asked whether CAFs expressing

Wnt3a could activate TOP-GFP in neighboring cancer cells, mimicking the actual TME *in vitro*. Cultures of CAFs expressing Wnt3a with cancer cells containing the TOP-GFP reporter resulted in Wnt activation in all cancer cell lines, including 067C (Fig. 1E, Supplementary Fig. S6B), which suggests that the presence of CAFs may augment activation.

Next, through media transfer (cancer or CAF donors → cancer TOP-GFP) we assessed whether activation requires cell-to-cell contact and confirmed the release of ligand from overexpressing cells (Supplementary Fig. S7A). Media transferred from $013CAF^{Wnt3a}$ to $013C^{TOP\text{-}GFP}$ activated TOP-GFP/Wnt signaling, demonstrating that released ligand was responsible for paracrine activation, which was blocked by Wnt inhibitors (Supplementary Fig. S7B–S7C). To confirm that TOP-GFP activation was not a result of an unrelated factor secreted by CAFs, we transferred $013C^{Wnt3a}$ media to $013C^{TOP\text{-}GFP}$ cells, which activated TOP-GFP, which was again blocked by Wnt inhibitors (Supplementary Fig. S7D).

We next tested whether Wnt3a overexpression activates Wnt signaling in CAFs. Forced Wnt3a expression resulted in limited detectable TOP-Flash activation only in 036CAFs only (Fig. 2A). However, Wnt3a increased *AXIN2* mRNA in all three CAF lines, as well as Axin2 and Nfat1 in 036CAF/067CAF and 013CAF/067CAF respectively (Supplementary Fig. S5C–S5D). Also, using the TOP-GFP reporter we observed paracrine signaling in all three CAF lines, whether co-cultured with CAFs or cancer cells expressing Wnt3a (Fig. 2B, Supplementary Fig. S6C).

3.5. Wnt3a ligand preferentially activate the Wnt pathway in cancer cells

To examine the timing of Wnt activation, 013CAFs simultaneously expressing an empty blue fluorescent protein (BFP) vector and TOP-GFP ($013CAF^{BFP/TOP\text{-}GFP}$) and 013Cs expressing TOP-GFP ($013C^{TOP\text{-}GFP}$) were seeded alone or co-cultured (1:1 ratio) and monitored via time lapse microscopy. rWnt3a induced TOP-GFP/Wnt activation in cancer cells first (~6 hours), followed by the activation of CAFs (~14 hours) (Fig. 3A). After 72 hours, nearly 90% of cancer cells were GFP-positive, regardless of whether they were cultured alone or with CAFs, while only 27% of CAFs cultured alone were GFP-positive, and co-cultured CAFs had a significantly smaller GFP-positive population (~13% (Fig. 3B). OMP-54F28 treatment increased the time to activation for CAFs (Fig. 3A) and significantly decreased the percentage of both GFP-positive cancer cells and CAFs (Fig. 3B–3C). OMP-18R5 significantly decreased the GFP-positive population in CAFs only (Fig. 3B–3C)

Next, to examine whether TOP-GFP activation/timing were affected by the source of Wnt3a, media was transferred from either $013C^{Wnt3a}$ or $013CAF^{Wnt3a}$ cultures. The timing of TOP-GFP activation for both cancer and CAF cells was similar to that observed with rWnt3a, with CAF activation somewhat slower ~18hrs. The source of Wnt3a (cancer, CAF) did not significantly alter the timing of TOP-GFP activation (Fig. 3D). Again, addition of OMP-54F28 delayed activation TOP-GFP in both 013C and 013CAF, regardless of the donor media (Fig. 3D). Media transfer generated fewer GFP-positive cancer cells (~19%) and CAFs (~5%) compared to rWnt3a, which likely allows for higher ligand concentrations. This positive population was again decreased with OMP-54F28 in both cancer and CAFs no matter the source of media (Fig. 3E–3F).

3.6. Wnt3a "primes" cancer cell invasiveness driven by CAFs

Prompted by increases in the EMT genes *TWIST1, SNAI1* and *ZEB1* in Wnt activated cancer cells (Supplementary Fig. S5A), we examined invasiveness using a modified *in vitro* Matrigel coated invasion assay (Fig. 4A). Wnt3a expression in 067C significantly increased invasiveness, while significantly fewer $013C^{Wnt3a}$ cells invaded compared to the $013C^{Empty}$ control (Fig. 4B). Addition of CAFs as chemoattractant for $013C^{Wnt3a}$ not only "rescued" the decrease seen with Wnt3a expression, but significantly increased 013^{Wnt3a} invasiveness compared to $013C^{Empty}$ cells (Fig. 4B). In contrast, the addition of 067CAF as chemoattractant decreased $067C^{Empty}$ invasiveness, which was further decreased by $067CAF^{Wnt3a}$, but the addition of CAFs as chemoattractant to $067C^{Wnt3a}$ cells had little effect. Similar to our TOP activation findings, Wnt16 expression in cancer cells or CAFs increased invasiveness of 067C (Supplementary Fig. S8A), while neither Wnt expression nor CAFs influenced the invasiveness of 036C (Fig. 4B).

To examine the individual contribution of cancer cells and CAFs to invasiveness, we mismatched chemoattractant CAFs, (e.g. 013C seeded with 067CAF). Consistent with previous results, Wnt3a expression decreased invasion by 013C when seeded with media alone (Supplementary Fig. S8B). Addition of chemoattractant 067CAF for $013C^{Empty}$ again increased invasiveness. Although the addition of 067CAF increased the invasiveness of $013C^{Wnt3a}$, this increase was much more modest than observed in paired 013C-013CAF assays (Fig. 4B). Finally, 013CAFs consistently had a negative effect on 067C invasion (Supplementary Fig. S8B).

We then assessed protein expression in 013C cells that actively invaded versus those that did not (cell scraping of membrane) when either media or 013CAF cells were used as chemoattractant. Regardless of chemoattractant, non-invading cells expressed significantly higher levels of Sox2 by densitometry (Fig. 4C, Supplementary Table S2), similar to previous results showing HNSCC CSCs to be highly epithelial [24]. Non-invading 013C cells exposed to both Wnt3a and CAFs as chemoattractant had dramatically upregulated Twist1, while Twist1 was decreased in invading cells under these conditions (Fig. 4B–4C, Supplementary Table S2). This suggests that Wnt3a exposure increases Twist1 levels at the same time 013C cells are "primed" to invade, but that Twist1 is again downregulated following CAF promoted invasion. Finally, we observed a decrease in E-cadherin when CAF media was transferred onto 013C cells, as well as expected increases in Nfat1 and Axin2 with exposure to Wnt3a (Supplementary Fig. S8C).

3.7. Activation of Wnt promotes further characteristics of stemness

CSCs direct invasion via their interaction with surrounding TME [25,37], and thus we investigated how Wnt affected CSC signaling and properties. *SOX2, OCT4, and NANOG* mRNA expression significantly increased in $013C^{Wnt3a}$ sphere cultures when compared to $013C^{Empty}$ controls (Fig. 5A). No change was observed in *SOX2* expression in $036C^{Wnt3a}$, and interestingly *SOX2* was decreased in $067C^{Wnt3a}$ (not shown). Sox2 protein levels in $013C^{Wnt3a}$ were dramatically increased by day 7 in non-adherent sphere cultures, along with increased levels of Nfat1 (Fig. 5B). Interestingly, on day 4 Oct4 was remarkably higher in $013C^{Wnt3a}$ then $013C^{Empty}$ cells but was lost by day 7 (Fig. 5B).

We next assessed Wnt activation induced phenotypic changes and found Wnt3a expression in 013C significantly increased Aldefluor activity (Fig. 5C) and sphere formation. Wnt3a expression in 067C and 036C did not induce significant differences in sphere size or number (Fig. 5D–5E), suggesting that robust Wnt activation in 013C by Wnt3a promotes a CSC-like phenotype. This is consistent with the observation that 013C cells are challenged to form spheres (CSC enrichment assay) had increased Wnt3a staining compared to 013C monolayer cultures (Supplementary Fig. S9A). However, we observed that rWnt16 expression in 067C cells activated Wnt/TOP-GFP (Supplementary Fig. S9B) and $067C^{Wnt16}$ spheres had increased nuclear β-catenin staining versus mock and empty vectors (Supplementary Fig. S9C), resulting in increased sphere formation and Sox2 expression (Supplementary Fig. S9D–S9F). Interestingly, Wnt16 expression in 013C decreased sphere formation by inducing a less structured, or "blebbing", phenotype and suppressed Sox2 (Supplementary Fig. S9D). Combined, these results suggested that Wnt signaling regulates the CSC phenotype in HNSCC but the process is cell line/ligand dependent (e.g. 013c/Wnt3a, 067C/Wnt16).

3.8. Targeting Wnt *in vivo* inhibits tumor growth

To assess Wnt inhibition *in vivo* mice bearing PDX tumors from four HNSCC cases (HPV-positive CUHN022 or HPV-negative CUHN044, CUHN036, or CUHN013) were treated with OMP-18R5 or OMP-54F28 (OncoMed Pharmaceuticals). We observed significant growth tumor inhibition with OMP-54F28 in CUHN044 and CUHN013, but observed greater inhibition with OMP-18R5 across all four cases (Fig. 6A). IHC analysis of control and treated tumor tissue showed significantly decreased post-treatment levels of Wnt3a and Axin2 in CUHN022, CUHN036, and CUHN044 (Fig. 6B). Wnt3a and Axin2 levels were not significantly changed in CUHN013 tumors following treatment.

3.9. Inhibiting Wnt in the TME blocks CSC tumor initiation

Having shown the effects of forced Wnt expression/signaling and the interplay between tumor and TME *in vitro*, we next inhibited endogenous Wnt signaling in highly tumorigenic HNSCC CSCs, such as in CUHN014 tumors, where as few as 10 $ALDH^{+}CD44^{high}$ cells readily generate tumors [24]. Mice bearing CUHN014 tumors, as well as mice that would be the recipient of CSC implantations, were treated for two weeks with vehicle or OMP-54F28 and continued treating CSC recipient mice two weeks following implantation. Recipient animals were pretreated to suppress baseline Wnt signaling as well as pathway upregulation upon CSC implantation (Fig. 6C). While treatment of the pre-sorted tumor decreased tumor formation, pre-treating recipient mice with Wnt inhibitor alone significantly blocked all tumor initiation (Fig. 6C). This effect was not as dramatic when both tumors and recipient mice were treated, suggesting that CSC tumor initiation requires Wnt signaling cues from the TME compartment (mouse recipient) upon implantation, and pretreatment of the tumor may allow for upregulation of alternative CSC pathways to compensate. Combined, these results suggest that Wnt signaling at the cancer-TME interface is critical for tumor growth (Fig. 6D).

4. DISCUSSION

Wnt is an oncogenic pathway in many tumors [8,17,18], but the role of the Wnt in the TME of HNSCC has been less firmly established. We observed enrichment of Wnt signaling and stem cell-related genes in advanced HNSCCs and found Wnt/CSC related protein expression to be highest at the cancer-TME interface. Human PDX tumor models are limited when investigating the cancer-TME interaction, particularly Wnt activation in HSNCC, due to loss of human TME components in immunocompromised mice [30]. To conduct mechanistic *in vitro* studies, we isolated paired cancer-CAF cell lines from the same patient tumors, allowing for manipulation of the Wnt pathway *in vitro*.

Wnt signaling is complex with three main pathways (one canonical, two non-canonical), as well as 19 ligands and 10 Fzd receptors that can stimulate activation [4]. Using 3D co-culture assays with cancer cells and CAFs to model the cancer-TME relationship *in vitro*, we observed upregulation of four ligands (Wnt2, Wnt3a, Wnt7a, Wnt16), identifying them as candidate HNSCC-promoters. We screened Wnt pathway activation by these ligands using TOP-Flash/GFP reporters and confirmed signaling by increased expression of Axin2 and Nfat1 [4,38]. We found that Wnt3a, which has demonstrated activity in several cancers [7,19,29], activated Wnt signaling in both cancer and CAF compartments of HNSCC.

Through co-culture and media-transfer experiments, we found that both CAFs and cancer cells exogenously expressing Wnt3a activate TOP-GFP in adjacent cells via paracrine signaling. As an exception, Wnt3a expression in 067Cs alone did not result in TOP-GFP expression, had an inhibitory effect, and decreased Axin2 expression. However, in the presence of CAFs+/−Wnt3a activated TOP-GFP in 067Cs, supporting our observation that robust Wnt signaling occurs primarily at the cancer-TME interface in tumor tissue. Finally, although 036C showed active Wnt signaling with Wnt3a expression, little to no downstream effect was seen in our functional assays (e.g. invasion, sphere formation).

The different responses by each cell line to Wnt3a is likely due to the sheer complexity of the Wnt signaling, as well as crosstalk with associated pathways (e.g. Hedgehog, Notch) [39]. Other explanations for the observed differences in activation between the three cell lines can be attributed to the availability of the Fzd receptor for Wnt3a and the presence of endogenous negative regulators such as DKK1, YAP/TAZ, and/or pathway promoters such as R-spondin [40–43]. Again, TOP-GFP was activated in 067C when co-cultured with CAFs and suggests that secondary factors released by CAFs augment Wnt activation, albeit we could not rule out differences in Wnt3a expression levels between CAFs and cancer cells. To this point, myofibroblasts (CAFs) have been shown to release hepatocyte growth factor (HGF), and HGF enhanced Wnt activity in colorectal cancer cells through secondary pathways [18]. Others have also reported differing responses with Wnt3a, where Wnt3a in breast cancer cells could either promote tumorigenesis or inhibit it, although the authors had not yet determined the underlying mechanisms [36]. Finally, others have observed the downstream effects of Wnt pathway signaling (i.e. EMT) even though Wnt pathway activation was not detectable [44], similar to the minimal TOP reporter activation we observe for 067^{Wnt16}.

We observed hallmarks of tumor promoting processes following Wnt ligand expression, such as an increased CSC phenotype following Wnt3a or Wnt16 expression in 013C and 067 respectively (Fig. 5, Supplementary Fig. S9). This suggests pathway activation is cell line/ligand dependent, but when the Wnt pathway results in promoting tumorigenesis or "stemness", the avenue that it goes through remains consistent. It is important to note that a single ligand (e.g. Wnt3a) may activate both canonical and non-canonical Wnt signaling [45], as we observed increased Nfat1 expression, a downstream read-out for non-canonical signaling. However, in these studies we focused on the downstream effects of canonical Wnt signaling, including the CSC phenotype.

To further investigate the importance of cancer-CAF interactions in Wnt signaling we studied the timing and frequency of TOP-GFP activation in cells alone and as co-cultures. Overall these results showed that cancer cells were preferentially activated by Wnt3a. Though not significant, media from CAF cultures activated TOP-GFP in recipient CAFs earlier than media from cancer cells, and we observed more GFP positive cancer cells treated with CAF^{Wnt3a} media, especially in cancer-CAF co-cultures. Also, OMP-54F28 significantly blocked GFP expression in cancer cells more when treated with CAF media. These observations all suggest CAF secreted factors are enhancing Wnt signaling. When taken together with our observations that Wnt signaling occurs primarily at the tumor stroma interface, as well as media transfer experiments showing Wnt3a from CAFs more readily activates TOP-GFP in cancer cells, this reasonably indicates a paracrine Wnt signaling loop. In this model, cancer cells would first become active and stimulate neighboring CAFs, which would enhance and maintain the Wnt signaling loop by continuing to activate cancer cells, providing the necessary sustaining Wnt signal needed in tumorigenesis (Fig. 6D).

Forced Wnt3a expression had contrasting effects on invasion, reducing it in 013Cs while increasing it in 067Cs, which is consistent with our results showing contrasting TOP/Wnt activation by Wnt3a in our cell lines. Decreased invasion by $013C^{Wnt3a}$ is inconsistent with other reports that Wnt signaling increases invasion [46,47]. However, we have an evolving understanding of the interplay between the CSC phenotype and EMT as well as the orchestration of invasion and ultimately metastasis. We recently demonstrated that HNSCC cells can undergo two distinct EMT events leading to either increased invasiveness/motility or resistance and increased CSC phenotype correlated with decreased invasiveness [48], consistent with what we are observing in the $013C^{Wnt3a}$.

We next tested invasiveness following Wnt3a expression in the presence of CAFs since the TME (CAFs) can promote invasion into surrounding normal tissue [37]. Using CAFs as chemoattractant increased invasion by 013Cs while decreasing 067C invasion. Remarkably, the decreased invasion observed in $013C^{Wnt3a}$ cells was rescued in the presence of 013CAFs, which increased invasion by $013C^{Wnt3a}$ cells more than that of control $013C^{Empty}$ cells. These findings suggested that although Wnt3a decreased invasion in 013C cells, Wnt3a "primed" cells to invade upon receiving proper cues from matched CAFs. Previous studies have shown that factors released from fibroblasts, including HGF, promote cancer cell invasion [49], possibly providing the tipping point in $013C^{Wnt3a}$ invasiveness. Importantly "unmatched" 067CAFs did not induce invasion in "primed" $013C^{Wnt3a}$ cells,

highlighting the inherent differences between cancer cells and CAFs that “evolved” together in the same patient and mismatched pairs.

To investigate the “priming” effects of Wnt3a we analyzed both non-invading and invading cells from the same populations. Expression of Sox2 in HNSCC cells induces an epithelial CSC-like phenotype [24], and suppression of Sox2 may be required for invasion. Wnt3a expressed in cancer cells themselves or chemoattractant CAFs increased Twist1 protein in non-invading cells. Media transferred from 013CAFs to $013C^{Wnt3a}$ cells decreased E-cadherin while increasing Axin2, and upon invasion, Twist1 and Sox2 were repressed. Also, HGF can stimulate Twist1, and Twist1 upregulation has been shown to be transient in relation to its function [50]. Together, these findings suggest that Wnt3a promotes an invasion-ready CSC-like phenotype through upregulation of Twist1 and Sox2, and upon receiving proper TME cues from CAFs, E-cadherin and Sox2 are suppressed, promoting invasion.

Wnt activation induced a traditional CSC phenotype, including Sox2 upregulation, ALDH activity and increased sphere formation. Interestingly and as stated above, similar phenotypic changes were induced by Wnt3a and Wnt16 in 013C and 067C cells respectively, but not vice versa. Prompted by the observation that Wnt promotes HNSCC stemness through Oct4 expression [7], we assessed its expression in non-adherent sphere culture. We found Oct4 was dramatically upregulated by day 4, however we also found that Sox2 levels were also increased by day 7 in $013C^{Wnt3a}$ cells compared to $013C^{Empty}$ controls, suggesting that Wnt may not only regulate Oct4 but also Sox2 in HNSCC. In a recent report on the role of PI3K and HNSCC CSC, we found that Sox2 regulates ALDH1A1 expression, increases resistance to therapy and promotes tumor growth [24], suggesting a downstream mechanism for Sox2 as well as a multifaceted role in tumor promotion. The timing of Oct4 and Sox2 upregulation, and the possibility of these two stemness factors regulating CSC at different stages warrants more study. Further confirming our observations, we observed increased Wnt3a staining in cells challenged to grow as spheres versus monolayer culture.

We also targeted Wnt *in vivo* using OMP-18R5 and OMP-54F28 in both HPV-negative (CUHN013, CUHN036, CUHN044) and HPV-positive (CUHN022) HNSCC PDX models. All four PDX cases significantly responded to OMP-18R5, while OMP-54F28 significantly inhibited growth in two of four models (CUHN044, CUHN022). The lack of response to OMP-54F28 in CUHN013 and CUHN036, may suggest that Wnt signaling in these cases is activated by ligands not readily sequestered by the peptide decoy. Decreased Wnt3a and Axin2 staining decreased with treatment, particularly in CUHN044 tumors that responded dramatically to both inhibitors. We did not observe any differences in response between HPV-negative and HPV-positive cases.

Lastly, we targeted the TME *in vivo* using OMP-54F28. Importantly, when the TME was treated with OMP-54F28 before CSC implantation, tumor initiation was significantly inhibited. Taken together, this data underlines the importance of treating both the tumor and TME compartments in cancer therapy. Although Wnt inhibition alone may not be sufficient

for tumor regression, in combination with chemotherapy and/or radiation, Wnt inhibition may suppress the CSCs, blocking tumor repopulation.

Supplementary Material

Refer to Web version on PubMed Central for supplementary material.

Acknowledgements

The authors wish to thank the patients who donated their tissue, blood and time, and to the clinical teams who facilitated patient informed consent, as well as sample and data acquisition. The authors wish to acknowledge Tim Hoey Ph.D. for insightful discussions and OncoMed Pharmaceuticals for enabling the utilization of their proprietary compounds.

Support

This work was supported by National Institutes of Health grants R01CA149456 (AJ), R21DE019712 (AJ), R01DE024371 (XJW and AJ), P30-CA046934 (University of Colorado Cancer Center Support Grant), P30-AR057212 (University of Colorado Skin Diseases Research Center Support Grant), DE020649 (XJW), Ruth L. Kirschstein National Research Service Award T32CA17468 (XJW; PNL trainee), Training in Otolaryngology Research T32DC012280 (CN trainee), the Daniel and Janet Mordecai Foundation (AJ), and the Peter and Rhonda Grant Foundation (AJ).

REFERENCES

1. Siegel RL, Miller KD, Jemal A. Cancer statistics, 2015. CA Cancer J Clin 2015;65(1):5–29. [PubMed: 25559415]
2. Chaturvedi AK, Engels EA, Pfeiffer RM et al. Human papillomavirus and rising oropharyngeal cancer incidence in the United States. J Clin Oncol 2011;29(32):4294–4301. [PubMed: 21969503]
3. Clevers H Wnt/beta-catenin signaling in development and disease. Cell 2006;127(3):469–480. [PubMed: 17081971]
4. Niehrs C The complex world of WNT receptor signalling. Nature reviews Molecular cell biology 2012;13(12):767–779. [PubMed: 23151663]
5. Shtutman M, Zhurinsky J, Simcha I et al. The cyclin D1 gene is a target of the beta-catenin/LEF-1 pathway. Proceedings of the National Academy of Sciences of the United States of America 1999;96(10):5522–5527. [PubMed: 10318916]
6. Watanabe O, Imamura H, Shimizu T et al. Expression of twist and wnt in human breast cancer. Anticancer research 2004;24(6):3851–3856. [PubMed: 15736421]
7. Lee SH, Koo BS, Kim JM et al. Wnt/beta-catenin signalling maintains self-renewal and tumourigenicity of head and neck squamous cell carcinoma stem-like cells by activating Oct4. The Journal of pathology 2014;234(1):99–107. [PubMed: 24871033]
8. White RA, Neiman JM, Reddi A et al. Epithelial stem cell mutations that promote squamous cell carcinoma metastasis. J Clin Invest 2013;123(10):4390–4404. [PubMed: 23999427]
9. Sakanaka C, Leong P, Xu L, Harrison SD, Williams LT. Casein kinase iepsilon in the wnt pathway: regulation of beta-catenin function. Proceedings of the National Academy of Sciences of the United States of America 1999;96(22):12548–12552. [PubMed: 10535959]
10. Aberle H, Bauer A, Stappert J, Kispert A, Kemler R. beta-catenin is a target for the ubiquitin-proteasome pathway. The EMBO journal 1997;16(13):3797–3804. [PubMed: 9233789]
11. Dann CE, Hsieh JC, Rattner A, Sharma D, Nathans J, Leahy DJ. Insights into Wnt binding and signalling from the structures of two Frizzled cysteine-rich domains. Nature 2001;412(6842):86–90. [PubMed: 11452312]
12. Pinson KI, Brennan J, Monkley S, Avery BJ, Skarnes WC. An LDL-receptor-related protein mediates Wnt signalling in mice. Nature 2000;407(6803):535–538. [PubMed: 11029008]

13. Lee JS, Ishimoto A, Yanagawa S. Characterization of mouse dishevelled (Dvl) proteins in Wnt/Wingless signaling pathway. The Journal of biological chemistry 1999;274(30):21464–21470. [PubMed: 10409711]
14. Rothbacher U, Laurent MN, Deardorff MA, Klein PS, Cho KW, Fraser SE. Dishevelled phosphorylation, subcellular localization and multimerization regulate its role in early embryogenesis. The EMBO journal 2000;19(5):1010–1022. [PubMed: 10698942]
15. Huber O, Korn R, McLaughlin J, Ohsugi M, Herrmann BG, Kemler R. Nuclear localization of beta-catenin by interaction with transcription factor LEF-1. Mechanisms of development 1996;59(1):3–10. [PubMed: 8892228]
16. Powell SM, Zilz N, Beazer-Barclay Y et al. APC mutations occur early during colorectal tumorigenesis. Nature 1992;359(6392):235–237. [PubMed: 1528264]
17. Kypta RM, Waxman J. Wnt/beta-catenin signalling in prostate cancer. Nature reviews Urology 2012;9(8):418–428. [PubMed: 22710668]
18. Vermeulen L, De Sousa EMF, van der Heijden M et al. Wnt activity defines colon cancer stem cells and is regulated by the microenvironment. Nat Cell Biol 2010;12(5):468–476. [PubMed: 20418870]
19. Bisson I, Prowse DM. WNT signaling regulates self-renewal and differentiation of prostate cancer cells with stem cell characteristics. Cell research 2009;19(6):683–697. [PubMed: 19365403]
20. Felthaus O, Ettl T, Gosau M et al. Cancer stem cell-like cells from a single cell of oral squamous carcinoma cell lines. Biochemical and biophysical research communications 2011;407(1):28–33. [PubMed: 21342656]
21. Yao CJ, Lai GM, Yeh CT et al. Honokiol Eliminates Human Oral Cancer Stem-Like Cells Accompanied with Suppression of Wnt/ beta -Catenin Signaling and Apoptosis Induction. Evidence-based complementary and alternative medicine : eCAM 2013;2013:146136. [PubMed: 23662112]
22. Warrier S, Bhuvanalakshmi G, Arfuso F, Rajan G, Millward M, Dharmarajan A. Cancer stem-like cells from head and neck cancers are chemosensitized by the Wnt antagonist, sFRP4, by inducing apoptosis, decreasing stemness, drug resistance and epithelial to mesenchymal transition. Cancer gene therapy 2014;21(9):381–388. [PubMed: 25104726]
23. Song J, Chang I, Chen Z, Kang M, Wang CY. Characterization of side populations in HNSCC: highly invasive, chemoresistant and abnormal Wnt signaling. PloS one 2010;5(7):e11456. [PubMed: 20625515]
24. Keysar SB, Le PN, Miller B et al. Regulation of Head and Neck Squamous Cancer Stem Cells by PI3K and SOX2. Journal of the National Cancer Institute 2017;109(1).
25. Cirri P, Chiarugi P. Cancer-associated-fibroblasts and tumour cells: a diabolic liaison driving cancer progression. Cancer metastasis reviews 2012;31(1–2):195–208. [PubMed: 22101652]
26. Sun Y, Campisi J, Higano C et al. Treatment-induced damage to the tumor microenvironment promotes prostate cancer therapy resistance through WNT16B. Nat Med 2012;18(9):1359–1368. [PubMed: 22863786]
27. Cheng Y, Phoon YP, Jin X et al. Wnt-C59 arrests stemness and suppresses growth of nasopharyngeal carcinoma in mice by inhibiting the Wnt pathway in the tumor microenvironment. Oncotarget 2015;6(16):14428–14439. [PubMed: 25980501]
28. Bhowmick NA, Neilson EG, Moses HL. Stromal fibroblasts in cancer initiation and progression. Nature 2004;432(7015):332–337. [PubMed: 15549095]
29. Gurney A, Axelrod F, Bond CJ et al. Wnt pathway inhibition via the targeting of Frizzled receptors results in decreased growth and tumorigenicity of human tumors. Proceedings of the National Academy of Sciences of the United States of America 2012;109(29):11717–11722. [PubMed: 22753465]
30. Keysar SB, Astling DP, Anderson RT et al. A patient tumor transplant model of squamous cell cancer identifies PI3K inhibitors as candidate therapeutics in defined molecular bins. Mol Oncol 2013;7(4):776–790. [PubMed: 23607916]
31. Bodnar AG, Ouellette M, Frolkis M et al. Extension of life-span by introduction of telomerase into normal human cells. Science 1998;279(5349):349–352. [PubMed: 9454332]

32. Dow LE, O'Rourke KP, Simon J et al. Apc Restoration Promotes Cellular Differentiation and Reestablishes Crypt Homeostasis in Colorectal Cancer. Cell 2015;161(7):1539–1552. [PubMed: 26091037]
33. Gunther EJ, Moody SE, Belka GK et al. Impact of p53 loss on reversal and recurrence of conditional Wnt-induced tumorigenesis. Genes Dev 2003;17(4):488–501. [PubMed: 12600942]
34. Le PN, McDermott JD, Jimeno A. Targeting the Wnt pathway in human cancers: Therapeutic targeting with a focus on OMP-54F28. Pharmacology & therapeutics 2014.
35. Hoey T. Development of FZD8-Fc (OMP-54F28), a Wnt signaling antagonist that inhibits tumor growth and reduces tumor initiating cell frequency.. AACR Annual Meeting.; Washington DC. 2013.
36. Green JL, La J, Yum KW et al. Paracrine Wnt signaling both promotes and inhibits human breast tumor growth. Proc Natl Acad Sci U S A 2013;110(17):6991–6996. [PubMed: 23559372]
37. Oskarsson T, Batlle E, Massague J. Metastatic stem cells: sources, niches, and vital pathways. Cell Stem Cell 2014;14(3):306–321. [PubMed: 24607405]
38. Jho EH, Zhang T, Domon C, Joo CK, Freund JN, Costantini F. Wnt/beta-catenin/Tcf signaling induces the transcription of Axin2, a negative regulator of the signaling pathway. Molecular and cellular biology 2002;22(4):1172–1183. [PubMed: 11809808]
39. Morris SL, Huang S. Crosstalk of the Wnt/beta-catenin pathway with other pathways in cancer cells. Genes & diseases 2016;3(1):41–47. [PubMed: 27081668]
40. Glinka A, Wu W, Delius H, Monaghan AP, Blumenstock C, Niehrs C. Dickkopf-1 is a member of a new family of secreted proteins and functions in head induction. Nature 1998;391(6665):357–362. [PubMed: 9450748]
41. Azzolin L, Panciera T, Soligo S et al. YAP/TAZ incorporation in the beta-catenin destruction complex orchestrates the Wnt response. Cell 2014;158(1):157–170. [PubMed: 24976009]
42. Kazanskaya O, Glinka A, del Barco Barrantes I, Stannek P, Niehrs C, Wu W. R-Spondin2 is a secreted activator of Wnt/beta-catenin signaling and is required for Xenopus myogenesis. Dev Cell 2004;7(4):525–534. [PubMed: 15469841]
43. Glinka A, Dolde C, Kirsch N et al. LGR4 and LGR5 are R-spondin receptors mediating Wnt/beta-catenin and Wnt/PCP signalling. EMBO Rep 2011;12(10):1055–1061. [PubMed: 21909076]
44. Wang Y, Bu F, Royer C et al. ASPP2 controls epithelial plasticity and inhibits metastasis through beta-catenin-dependent regulation of ZEB1. Nat Cell Biol 2014;16(11):1092–1104. [PubMed: 25344754]
45. Tu X, Joeng KS, Nakayama KI et al. Noncanonical Wnt signaling through G protein-linked PKCdelta activation promotes bone formation. Dev Cell 2007;12(1):113–127. [PubMed: 17199045]
46. Goto M, Mitra RS, Liu M et al. Rap1 stabilizes beta-catenin and enhances beta-catenin-dependent transcription and invasion in squamous cell carcinoma of the head and neck. Clin Cancer Res 2010;16(1):65–76. [PubMed: 20028760]
47. Wu Y, Ginther C, Kim J et al. Expression of Wnt3 activates Wnt/beta-catenin pathway and promotes EMT-like phenotype in trastuzumab-resistant HER2-overexpressing breast cancer cells. Molecular cancer research : MCR 2012;10(12):1597–1606. [PubMed: 23071104]
48. Keysar SB, Le PN, Anderson RT et al. Hedgehog Signaling Alters Reliance on EGF Receptor Signaling and Mediates Anti-EGFR Therapeutic Resistance in Head and Neck Cancer. Cancer Res 2013;73(11):3381–3392. [PubMed: 23576557]
49. Lewis MP, Lygoe KA, Nystrom ML et al. Tumour-derived TGF-beta1 modulates myofibroblast differentiation and promotes HGF/SF-dependent invasion of squamous carcinoma cells. Br J Cancer 2004;90(4):822–832. [PubMed: 14970860]
50. Bendinelli P, Maroni P, Matteucci E, Desiderio MA. HGF and TGFbeta1 differently influenced Wwox regulatory function on Twist program for mesenchymal-epithelial transition in bone metastatic versus parental breast carcinoma cells. Mol Cancer 2015;14:112. [PubMed: 26041563]

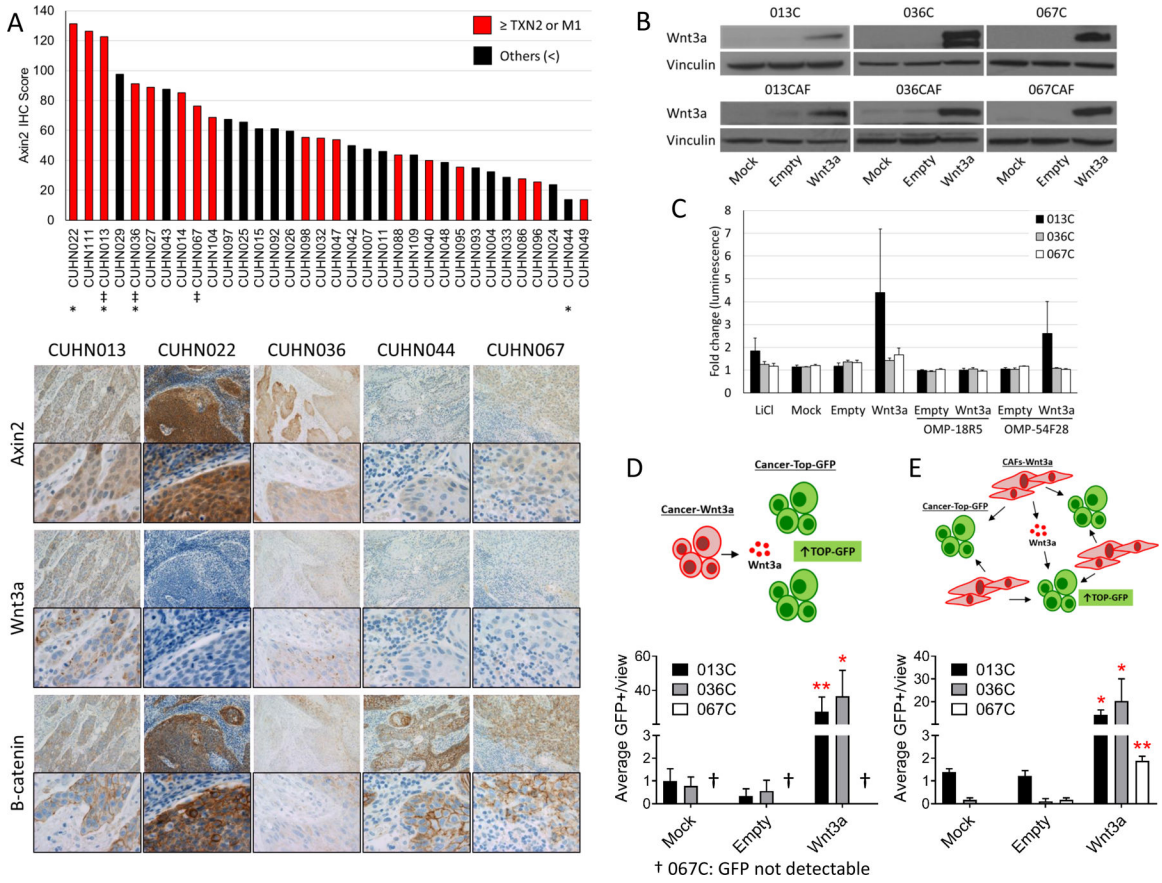

Figure 1. Wnt signaling in HNSCC tumors and cell lines.

(A) HNSCC patient tissue was stained (IHC) for Axin2. Eight of the highest ten Axin2 expressing tumors had advanced TNM stage (≥TXN2 or M1); the overall trend was not significant. (‡= HNSCC cell line cases, *= PDX cases used in efficacy studies). Wnt3a, β-catenin, and Axin2 staining intensity is consistently highest at the tumor-stroma interface in HNSCC patient samples (Top= 10X, Bottom with border= 40X). **(B)** Western blots confirm Wnt3a protein overexpression in all matched cancer and CAF cell lines. **(C)** 013C^{Wnt3a} cells activated the TOP-Flash reporter, which was suppressed by the addition of Wnt inhibitors (OMP-18R5, OMP-54F28). Activation of TOP-Flash by 036C^{Wnt3a} and 067C^{Wnt3a} cells was both low and variable (not shown). **(D)** Co-culture of TOP-GFP (reporter) cancer cells with those expressing Wnt3a. Cells were co-cultured at three different ratios (1 Cancer$^{TOP-GFP}$:1 Cancer^{Wnt3a}, 1:4 and 1:10) in order to test different ligand availability. With co-culture, Wnt activity (GFP-positive cells) was observed in 013C and 036C cells. GFP was not detectable in 067C no matter the ratio or number of days of incubation. GFP-positive cells were quantified per microscope viewing field due to equivalent cell densities. **(E)** CAFs were co-cultured with their respective cancer pairs and similarly seeded at the three different ratios stated above. Using this co-culturing method, we show paracrine signaling wherein Wnt3a overexpressing CAFs can activate Wnt signaling in cancer cells containing the TOP-GFP reporter for all 3 cancer cells. GFP positive cells were quantified per view. *= $P \leq .05$, **= $P \leq .01$.

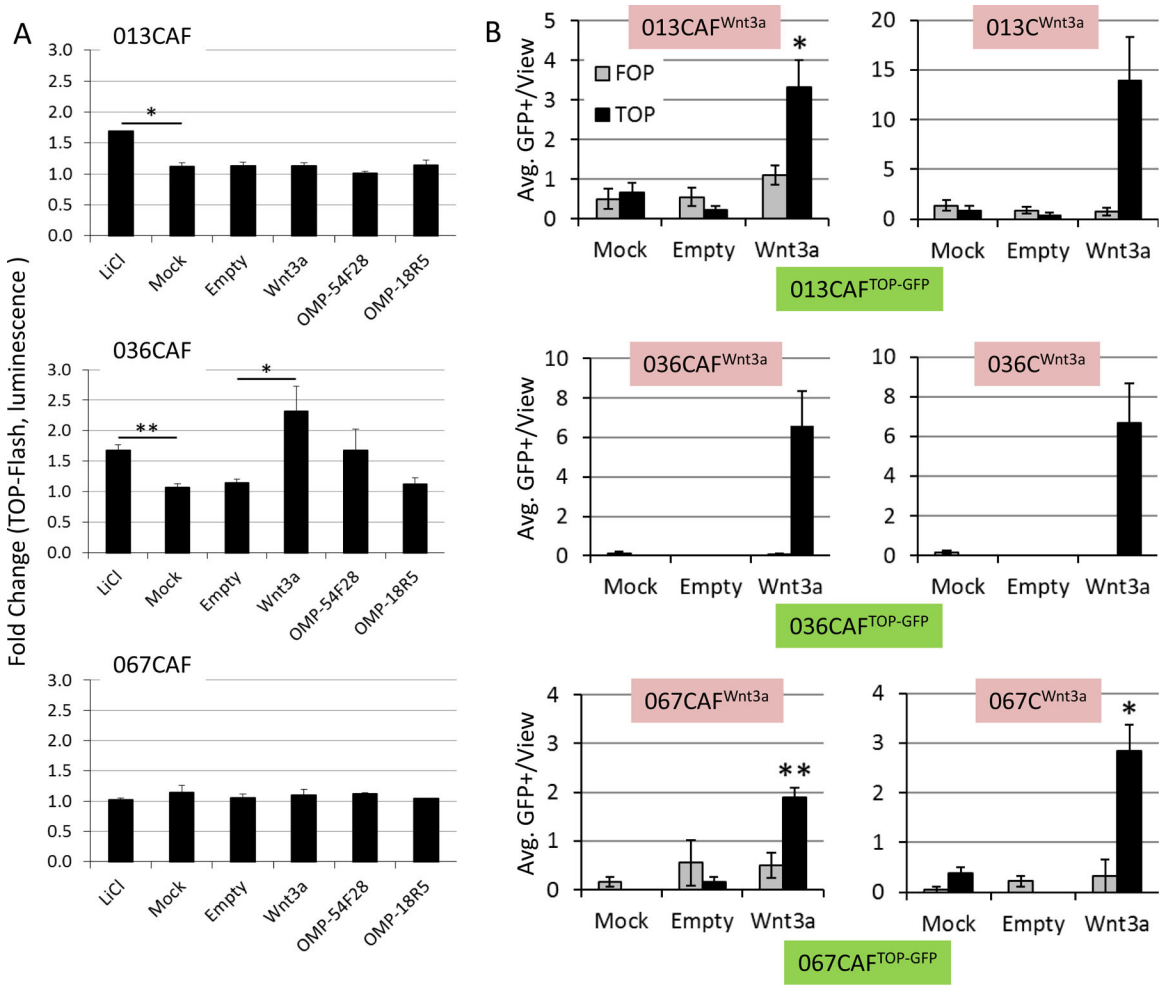

Figure 2. The Wnt3a ligand also activates Wnt signaling in HNSCC CAFs.

(A) Wnt activity was not detectable by the TOP-Flash reporter in 067CAFs and 013CAFs, with some luciferase activity observed in 036CAFs. **(B)** Wnt3a overexpressing cells (red/top cell line), either CAFs or cancer cells, were co-cultured with CAFs containing the TOP-GFP reporter (green/bottom cell line). Wnt3a expression effectively activated Wnt signaling (TOP-GFP) in adjacent CAFs. The TOP-GFP assay was quantified by counting GFP-positive cells per view due to equivalent cell densities. All three CAF cell lines had increased GFP-positive cells when co-cultured with Wnt3a expressing cells (cancer or CAF). *= $P \leq .05$, **= $P \leq .01$.

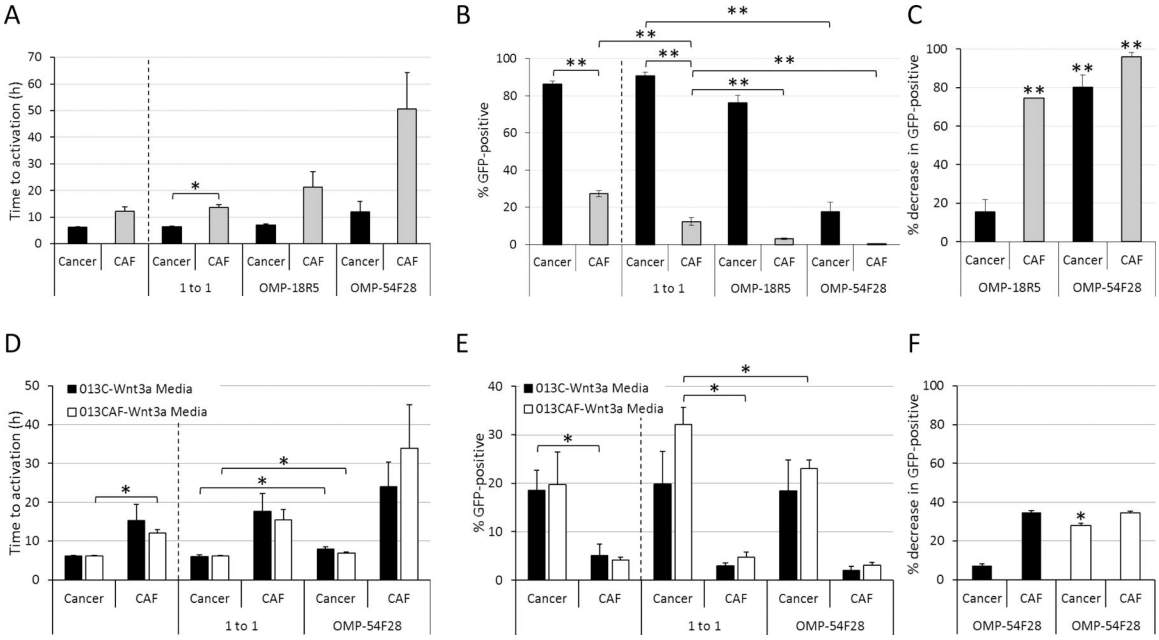

Figure 3. Preferential Wnt activation of cancer cells by Wnt3a.

(A) Elapsed time to activation of TOP-GFP in 013C and 013CAF cells following exposure to rWnt3a. Cells left of the dashed lines were seeded alone while all assayed cells to the right of the dashed line were seeded at a 1:1 ratio of cancer:CAFs. **(B)** Percentage of 013C and 13CAF cells that are TOP-GFP-positive at 72 hours following addition of rWnt3a. Cells left of the dashed line were seeded alone while all assayed cells to the right of the dashed line were seeded at a 1:1 ratio of cancer:CAFs. **(C)** Change in the percentage of GFP-positive cells in cultures containing inhibitors OMP-18R5 and OMP54F-28 compared to controls (Fig. 3B). **(D)** Elapsed time to activation of TOP-GFP for 013C and 013CAF cells following transfer of media from either $013C^{Wnt3a}$ or $013CAF^{Wnt3a}$. Cells left of the dashed line were seeded alone while all assayed cells to the right of the dashed line were seeded at a 1:1 ratio of cancer:CAFs. **(E)** Percentage of 013C and 013CAF cells that are TOP-GFP-positive at 72 hours following media transfers from cancer cells or CAFs expressing Wnt3a. Cells left of the dashed line were seeded alone while all assayed cells to the right of the dashed line were seeded at a 1:1 ratio of cancer:CAFs. **(F)** Change in the percentage of GFP-positive cells in cultures following media transfer and with OMP-18R5 and OMP54F-28 compared to controls (Fig. 3E). *= $P \leq .05$, **= $P \leq .01$.

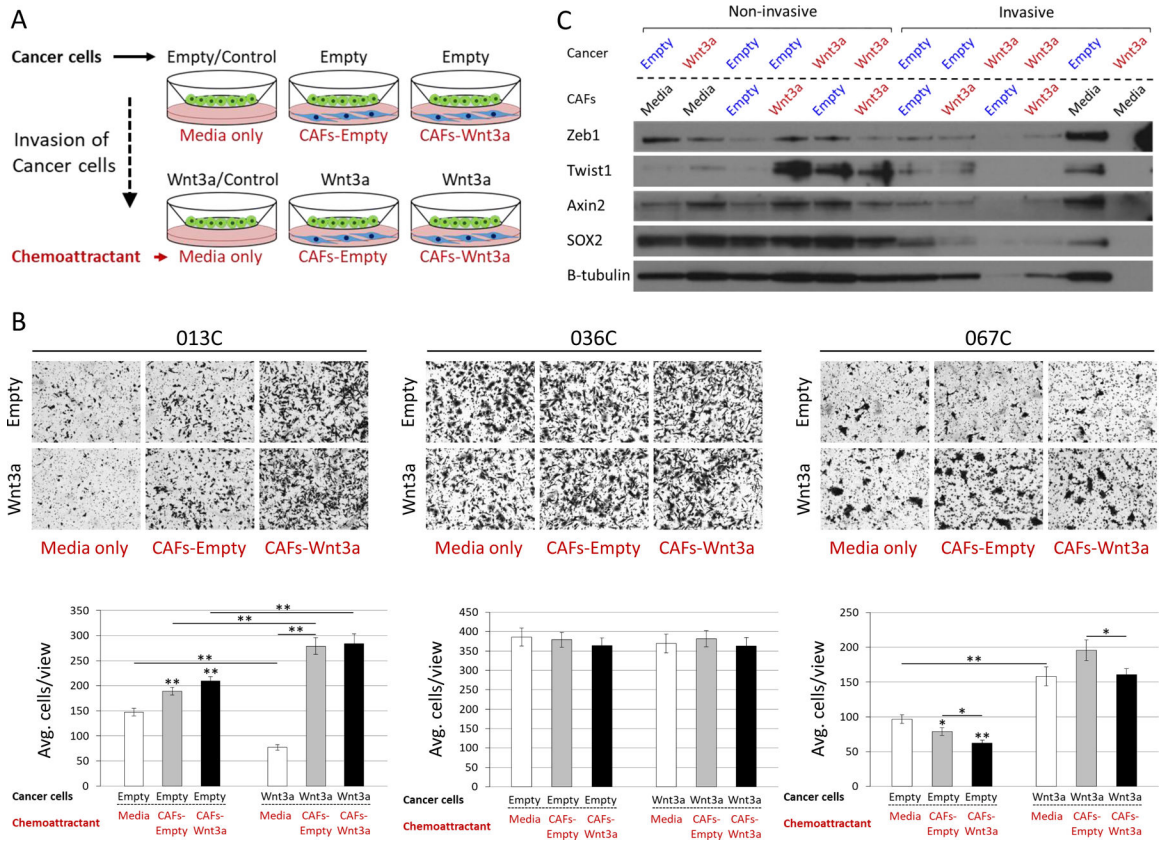

Figure 4. Wnt3a primes cancer cells for invasion that is initiated in the presence of CAFs.

(A) Schemata of the modified Matrigel invasion assay design. Cancer cells were seeded in the insert well of Matrigel invasion chambers while CAFs were seeded on the bottom well as a chemoattractant. Media containing 10% FBS was used a baseline control. **(B)** Invasion was decreased in $013C^{Wnt3a}$ cells when compared to control $013C^{Empty}$ cells at baseline, but the addition of CAFs as chemoattractant increased the invasiveness of all cancer cells. Importantly, $013C^{Wnt3a}$ were more greatly affected by the addition of CAFs compared to control $013C^{Empty}$ cells. Invasiveness was increased in $067C^{Wnt3a}$ at baseline. CAFs as a chemoattractant decreased invasion by $067C^{Empty3a}$control cells. However, this decrease was "rescued" with the addition of CAFs in 067C cells expressing Wnt3a (067^{Wnt3a}.). Neither Wnt3a or CAFs altered the invasiveness of 036C cells**. (C)** Protein expression of non-invasive and invasive cells (scraped from the bottom of the Matrigel membrane) with varying chemoattractant (Media, CAF-Empty, CAF-Wnt3a). *= $P \leq .05$, **= $P \leq .01$.

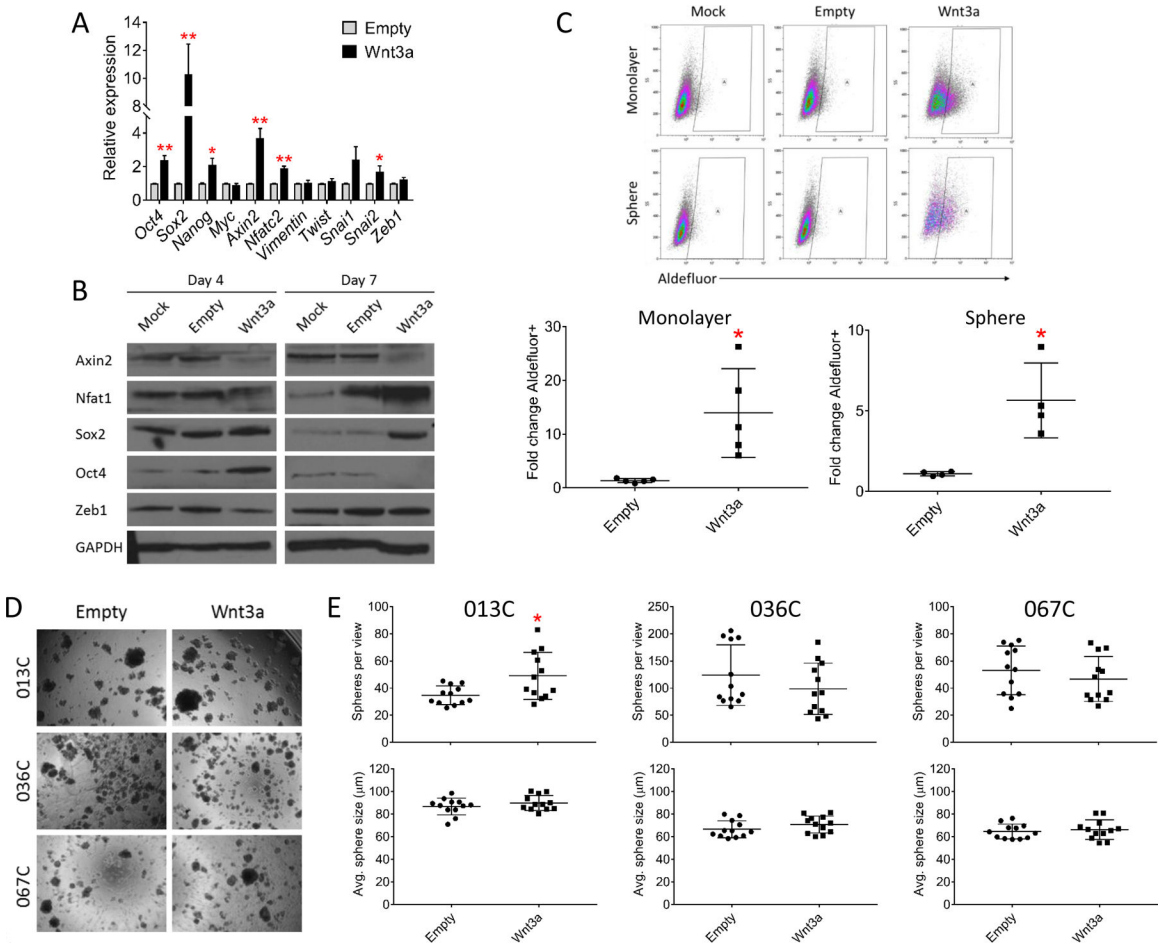

Figure 5. Wnt3a expression and Wnt signaling pathway activation increases characteristics of CSCs.

(A) Exogenous Wnt3a expression significantly increases expression of CSC-related (*Sox2*, *Oct4*, *Nanog*), Wnt-related (*Axin2*, *Nfatc2*), and EMT-related (*Snai2* genes in 013C cells. **(B)** Oct4 and Sox2 protein levels are increased in sphere cultures of $013C^{Wnt3a}$ cells on days four and seven respectively. **(C)** Wnt pathway activation significantly increases the $ALDH^{+}$ population in both monolayer and sphere cultures of 013C. (**D and E**) Wnt3a expression in increases sphere formation in 013C. No significant change in sphere size or number was observed in 067C or 036C cells expressing Wnt3a, even though Wnt3a forced expression also activated TOP-GFP 036C cells as previously described. *= $P \leq .05$, **= $P \leq .01$.

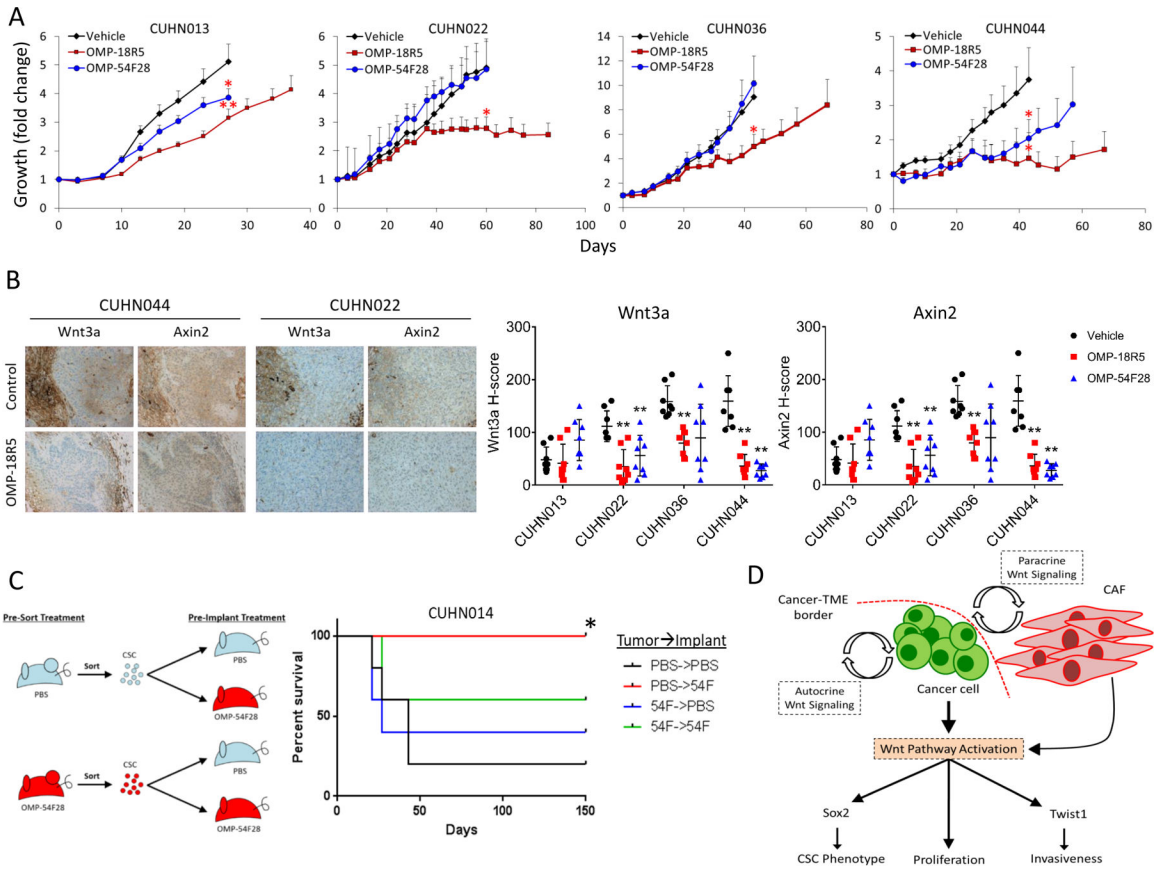

Figure 6. Wnt inhibition blocks HNSCC PDX tumor proliferation *in vivo*.

(A) Mice bearing HNSCC PDX tumors were treated every two weeks with Wnt inhibitors OMP-18R5 and OMP-54F28. Control tumors were harvested upon reaching 2,000mm^3. OMP-18R5 significantly inhibited tumor growth in all four PDX models, while OMP-54F24 significantly inhibited growth in only CUHN013 and CUHN044. **(B)** Decreased Wnt3a and Axin2 staining in OMP-18R5 treated PDX tumors by IHC and H-score analysis. **(C)** Pretreatment of recipient mice with the Wnt ligand scavenger OMP-54F28, compared to PBS control animals, significantly (P=.048) blocked tumor growth by CSCs sorted from PDX tumors. **(D)** Conceptual model of cancer-TME interaction and its role in tumor progression. *= $P \leq .05$, **= $P \leq .01$.